Engineering-Specific Pharmacological Binding Sites for Peptidyl Inhibitors of Potassium Channels into KcsA†

Christian Legros,*,‡,§ Christian Schulze,‡ Maria L. Garcia,|| Pierre E. Bougis,⊥ Marie-France Martin-Eauclaire,⊥ and Olaf Pongs‡

Institut für Neurale Signalverarbeitung, ZMNH, Universität Hamburg, Martinistrasse 52, D-20246 Hamburg, Germany, Department of Ion Channels, Merck Research Laboratories R80N-C31, P.O. Box 2000, Rahway, New Jersey 07065, and CNRS UMR 6560, Ingénierie des Protéines, Institut Fédératif de Recherche Jean Roche, Université de la Méditerranée, Laboratoire de Biochimie, Faculté de Médecine Secteur Nord, Bd. Pierre Dramard, F-13916 Marseille Cedex 20, France

Received June 7, 2002; Revised Manuscript Received October 23, 2002

ABSTRACT: The bacterial potassium channel, KcsA, can be modified to express a high-affinity receptor site for the scorpion toxin kaliotoxin (KTX) by substituting subregion I in the P region of KcsA with the one present in the human voltage-gated potassium channel Kv1.3 [Legros, C., Pollmann, V., Knaus, H. G., Farrell, A. M., Darbon, H., Bougis, P. E., Martin-Eauclaire, M. F., and Pongs, O. (2000) *J. Biol. Chem. 275*, 16918−16924]. This approach opened the way to investigate whether sequence differences in subregion I of Kv1 channels correlate with the distinct pharmacological profiles of peptide inhibitors. A panel of six chimeras between KcsA and human Kv1.1−6 were constructed, expressed in *Escherichia coli*, purified to homogeneity, and assessed in filter binding assays using either monoiodo-tyrosine-KTX ([^{125}I]KTX) or monoiodo-tyrosine-hongotoxin$_1$(A19Y/Y37F) ([^{125}I]HgTX$_1$(A19Y/Y37F)). The KcsA−Kv1.X chimeras were found to have lower affinities for these ligands than the corresponding mammalian Kv1.X channels, indicating that other parts of the channels may contribute to binding or that subtle structural differences exist between these channels. The properties of the KcsA−Kv1.X chimeras were also characterized in surface plasmon resonance experiments. KcsA−Kv1.3 chimeras were immobilized on the surface of a sensor chip for determining, in real time, binding of the peptides. KTX binding properties to immobilized KcsA−Kv1.3 chimera were similar to those determined by filtration techniques. Taken together, our results demonstrate that the pharmacological profile of peptide toxins can be incorporated into KcsA−Kv1.X chimeras containing the subregion I of the corresponding mammalian Kv1.X channels. This innovative approach may facilitate the high-throughput screening of ligand libraries aimed at the discovery of novel potassium channel modulators.

Voltage-gated potassium channels (Kv)[1] belong to a highly diverse superfamily whose members participate in many important physiological functions (*1*). A number of these ion channels are associated with hereditary human diseases [e.g., the long QT-syndrome (*2*)]. Given the diversity of potassium channels and their importance for regulation of cellular excitability and signaling, potassium channels represent a target of interest for the development of novel and useful therapeutic agents with a wide range of clinical applications. Thus, it would be desirable to produce potassium channels in a form that would make them easily accessible to mine for channel modulators.

The crystal structure of the KcsA potassium channel has been solved, providing the first three-dimensional structure of a potassium channel at atomic resolution (*3*, *4*). KcsA is a tetramer with 4-fold symmetry around a central pore made up by amino acid residues of the P region. The outer vestibule contains a groove formed by turrets present on the amino-terminal side of the P region. This vestibule serves as the receptor site for a number of potassium channel blockers [i.e., peptides derived from scorpion, snake, spider venoms, and sea anemone] as well as small organic molecules such as TEA (*5*). Although KcsA is not sensitive to peptidyl inhibitors of mammalian Kv1 channels, some of the peptide binding properties of eukaryotic Kv1 channels have been transferred to KcsA by mutating certain residues in the outer vestibule of that channel. These studies have helped to advance our understanding of those structural aspects involved in the interaction of peptide inhibitors with the vestibule of eukaryotic Kv channels (*6*, *7*).

† This work was supported in part by the Bundesministerium für Bildung und Forschung, the Deutsche Akademische Austauschdienst (O.P.), and the PROCOPE program (P.M.).

* To whom correspondence should be addressed. Phone: +33 (0) 1 69 47 76 45; fax: +33 (0) 1 69 47 76 55; e-mail: christian.legros@chimie.univ-evry.fr.

‡ Universität Hamburg.

§ Present address: CNRS UMR 8587, Laboratoire Analyse et Environnement, Institut des Sciences, Université d'Evry Val-d'Essonne, Bd. François Mittérand, F-91025 Evry Cedex, France.

|| Merck Research Laboratories.

⊥ Université de la Méditerranée.

[1] Abbreviations: Kv, voltage-gated K^+ (channel); ChTX, charybdotoxin; DM, *n*-decyl-*β*-D-maltopyranoside; HgTX$_1$, hongotoxin 1; KTX, kaliotoxin; [^{125}I]HgTX$_1$(A19Y/Y37F), monoiodotyrosine hongotoxin 1 (A19Y/Y37F); [^{125}I]KTX, monoiodotyrosine kaliotoxin; SPR, surface plasmon resonance; EC_{50}, molar concentration that produces 50% of the maximum possible response; IC_{50}, molar concentration that reduces the specific binding of a radioligand by 50%; K_d, equilibrium dissociation constant; K_i, equilibrium inhibition constant; k_{on}, association rate constant; k_{off}, dissociation rate constant; k_t, coefficient of mass transfer.

10.1021/bi026264a CCC: $22.00
Published on Web 11/27/2002

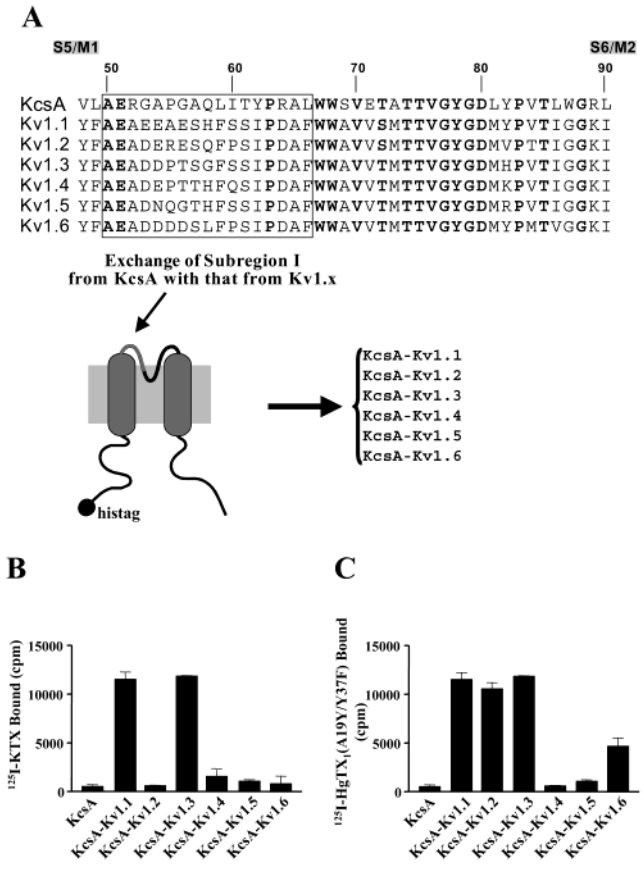

FIGURE 1: Binding of [^{125}I]KTX and [^{125}I]HgTX$_1$(A19Y/Y37F) to KcsA−Kv1.X chimeras. (A) Schematic diagram showing the alignment of residues in the S5/M1−S6/M2 linker of KcsA (residues 48−90) and hKv1.1−hKv1.6 subunits. Conserved amino acid residues are represented in bold. A His tag was added at the N-terminus of each construct to facilitate purification. Subregion I, which was transferred to KcsA to generate the different chimeras, is framed. Purified KcsA−Kv1.X channels were assayed in filtration binding assays with either [^{125}I]KTX (B) or [^{125}I]HgTX$_1$(A19Y/Y37F) (C). Vertical bars represent the SEM for each experimental point.

We have previously shown that substitution of two subregions in the KcsA P region (subregions I and III) by the respective P region sequences of the human Kv1.3 channel reconstitutes a high-affinity receptor on KcsA for the scorpion peptide kaliotoxin (KTX) (*7*). Subregion I contains the turret that could be involved in conferring specificity to the peptide/channel interaction. For instance, two peptides of the charybdotoxin superfamily, KTX and hongotoxin$_1$(A19Y/Y37F) (HgTX$_1$(A19Y/Y37F)), display different specificities for members of the Kv1 channel family (*8*, *9*). KTX blocks Kv1.1 and Kv1.3 but not Kv1.2, Kv1.4, Kv1.5, and Kv1.6 channels (*8*), whereas HgTX$_1$(A19Y/Y37F) blocks with very high potency Kv1.1, Kv1.2, Kv1.3, and Kv1.6 channels, but it does not block Kv1.4 and Kv1.5 channels (*9*).

To investigate whether sequence differences in subregion I correlate with the pharmacological profile of Kv1 channels, chimeric channels were constructed by replacing KcsA subregion I by the corresponding subregions I of human Kv1.1−Kv1.6 channels (Figure 1A). Binding of [^{125}I]KTX and [^{125}I]HgTX$_1$(A19Y/Y37F) to the KcsA−Kv1.X chimeras was characterized using filtration techniques. A novel nonradioactive binding assay was also developed in which KcsA−Kv1.X chimeras are covalently linked to an inert surface and assayed with surface plasmon resonance (SPR) for peptide binding. Taken together, our data indicate that subregion I of Kv1 channels is a major contributor to the pharmacological profile of native channels.

EXPERIMENTAL PROCEDURES

Materials. Production of recombinant proteins in *Escherichia coli* strains was carried out in SB medium (25 g/L bactotryptone, 15 g/L bactoyeast extract, 5 g/L NaCl, 0.1% D-glucose, pH 7.0). Ampicillin and kanamycin (Sigma) were added to final concentrations of 100 and 25 μg/mL, respectively. IPTG was from Roth. DM was purchased from Calbiochem. *E. coli* XL1-Blue (Stratagene) served as host for the propagation of pQE-32 (Qiagen) and constructs; *E. coli* M15 [pREP4] (Qiagen) was used for the production of recombinant proteins. Glass fiber filters were obtained from Whatman. CM5 dextran chips and the amine-coupling kit containing EDC and NHS were purchased from BIAcore (Sweden). All other reagents were obtained from Stratagene, Sigma, Fluka, or Merck.

Construction of KcsA−Kv1.X Chimeras. Chimeric constructs consisting of the core of KcsA and part of the pore-forming loop of either hKv1.1, hKv1.2, hKv1.4, hKv1.5, or hKv1.6 were prepared using standard PCR techniques. The KcsA−Kv1.3 chimera has been previously described (*7*). A His tag was added to the N-terminus of each protein to allow purification by immobilized-metal-affinity chromatography. All constructs were sequenced using an ABI 377 DNA sequencer.

Induction and Purification of KcsA Wild-Type and KcsA−Kv1.X Chimeras. Recombinant chimeric channels were expressed and purified as described (*7*) with minor modifications. The expression of recombinant proteins was achieved by addition of 0.4−0.5 mM IPTG for 2−3 h after OD_{600nm} reached 1−2 absorbance units. Protein concentrations were determined by spectrophotometry and the microBCA test (Pierce). Proteins were analyzed by SDS−PAGE (*10*).

Binding Studies. [^{125}I]KTX and [^{125}I]HgTX$_1$(A19Y/Y37F) were prepared as previously described (*9*, *11*). All binding experiments were performed at room temperature. For [^{125}I]-KTX binding experiments, the binding buffer consisted of 20 mM Tris-HCl (pH 7.4), 50 mM NaCl, and 0.1% bovine serum albumin (buffer A). For [^{125}I]HgTX$_1$(A19Y/Y37F) binding experiments, 3 mM of KCl was added to buffer A. In experiments with purified proteins, 2 mM DM was also present in the incubation media. At the end of the incubation period, the reaction was stopped by addition of 4 mL of ice-cold 20 mM Tris-HCl (pH 7.4), 150 mM NaCl, and samples were filtered through GF/C glass fiber filters presoaked in 0.5% polyethylenimine. Filters were washed twice with 4 mL of buffer. Nonspecific binding was defined in the presence of 100 nM unlabeled peptide. For each experiment, triplicate or duplicate assays were carried out, and the data were averaged.

Analysis of Data. Data obtained from radioligand binding experiments were analyzed by nonlinear regression and linear regression analysis using PRISM software (GraphPad) as previously described (*7*). When ligand depletion occurred, the following equation was used to determine K_d and B_{max} values:

$$B_{tot} = B_{max} \times L_f/(K_d + L_f) + L_f \times NS$$

where B_{tot} represents the amount of bound ligand, L_f is the concentration of free ligand, B_{max} is the maximum receptor concentration, K_d is the equilibrium dissociation constant, and NS is the degree of nonspecific binding determined in the presence of excess of unlabeled peptide (*12*).

SPR Experiments. All determinations were carried out using a BIAcore 3000 instrument (Biacore, Sweden) with sensor chips maintained at 25 °C (*13*). The running buffer consisted of 10 mM sodium phosphate, 150 mM NaCl, 3 mM KCl, and 2 mM DM, pH 7.0. Proteins were covalently immobilized onto CM5 dextran sensor chips via primary amino groups, using a standard coupling protocol (*14*). In brief, the sensor surface was activated by a 7-min pulse of 0.2 M 1-ethyl-3(3-dimethylaminopropyl)carbodiimide hydrochloride and 50 mM *N*-hydroxysuccinimide. A protein solution (0.3 mg/mL in 10 mM sodium acetate, pH 5.2) was then injected for 5−10 min. Ethanolamine (1 M, pH 8.5) was used to block the remaining activated carboxyl groups. Ligand densities of 100−150 fmol/mm^2 were reached. Flow cell 1 was used as a blank surface. Regeneration of the sensor chip was achieved with three pulses of 1 M KCl. Corresponding peptides were injected at 10 μL/min. All sensorgrams were corrected for background and bulk refractive index by subtracting the reference flow cell signal. The 1:1 Langmuir binding interaction model was used to fit the data. Data were analyzed using the BIA evaluation 3.0 software (Biacore).

RESULTS

Previous studies using chimeras of the pore region of KcsA and the Kv1.3 channel have indicated that an important region of the channel for interaction with KTX corresponds to subregion I of the P region (SIP region) in the Kv1.3 channel (Figure 1A) (*7*). Interestingly, the SIP region of members of the Kv1 channel family shows a high degree of sequence variation, whereas the rest of the P region sequence is relatively invariant (Figure 1A). Since Kv1.X channels have distinct sensitivities toward pore-blocking peptidyl inhibitors, we hypothesized that differences in the SIP sequences could account for the different pharmacological profiles of these Kv1 channels. We tested the hypothesis by investigating [^{125}I]KTX and [^{125}I]HgTX$_1$(A19Y/Y37F) binding to a panel of KcsA−Kv1.X chimeras.

SIP Sequences of Kv1 Channels Define Binding Specificity to Peptidyl Inhibitors. Chimeric KcsA−Kv1.X proteins (Figure 1A) were expressed and purified from *E. coli* (see Experimental Procedures). Purified proteins behaved as tetramers in SDS−PAGE (data not shown). In the case of KcsA and KcsA−Kv1.3, we obtained yields of 2−2.5 mg of purified protein per liter of *E. coli* culture. In contrast, expression of the other chimeras yielded relatively low amounts of purified protein (0.05−0.3 mg/L). The properties of purified chimeric proteins were characterized in binding assays using either [^{125}I]KTX or [^{125}I]HgTX$_1$(A19Y/Y37F) (Figure 1B,C). Purified wild-type KcsA channel preparations served as specificity controls. In addition to KcsA−Kv1.3 (*7*), [^{125}I]KTX binding was also observed with KcsA−Kv1.1 (Figure 1B), whereas the other chimeras (KcsA−Kv1.2, KcsA−Kv1.4, KcsA−Kv1.5, and KcsA−Kv1.6) did not bind [^{125}I]KTX (Figure 1B).

[^{125}I]HgTX$_1$(A19Y/Y37F) bound to KcsA−Kv1.1, KcsA−Kv1.2, KcsA−Kv1.3, and KcsA−Kv1.6 but not to KcsA−Kv1.4 and KcsA−Kv1.5 chimeras (Figure 1C). The results of these binding assays indicated that the KcsA−Kv1.X chimeras qualitatively mirror the pharmacological specificities reported for the respective mammalian Kv1 channels (*8*, *9*).

[^{125}I]KTX Binding to the KcsA−Kv1.1 Chimera. Under equilibrium conditions, specific binding of [^{125}I]KTX to KcsA−Kv1.1 was saturable (Figure 2A), and the data could be fitted to a single binding isotherm with a K_d of 3.2 nM and a B_{max} of 1.6 fmol/ng of purified protein. This B_{max} value is ∼8-fold lower than the expected theoretical B_{max} of 12.3 fmol/ng protein, suggesting that only ∼13% of the KcsA−Kv1.1 protein binds [^{125}I]KTX. The relatively low activity of the KcsA−Kv1.1 chimera was consistently observed in all our protein preparations. Changes in the detergent used in the solubilization procedure did not improve the yield of active KcsA−Kv1.1 protein (data not shown). Both membrane and purified KcsA−Kv1.1 preparations displayed identical affinities for KTX in competition binding experiments, K_i values of 3.6 and 3.9 nM, respectively (Figure 2B), indicating that the solubilization and purification procedure did not alter the affinity of KTX for the KcsA−Kv1.1 chimera. Interestingly, [^{125}I]KTX displays a 10−20-fold higher affinity for the KcsA−Kv1.3 chimera (*7*).

The kinetics of [^{125}I]KTX association and dissociation was also determined (Figure 2C,D). Binding of [^{125}I]KTX to KcsA−Kv1.1 reached equilibrium after ∼2 h incubation. Data could be fitted to a single bimolecular binding reaction, for which an association rate constant, k_{on}, of 3.1×10^5 M^{-1} s^{-1} was determined (inset, Figure 2C). Dissociation of [^{125}I]-KTX from KcsA−Kv1.1, initiated by addition of 50 nM unlabeled KTX, followed monoexponential kinetics (Figure 2D), indicative of a first-order reaction, with a k_{off} of 0.00083 s^{-1}, corresponding to a halflife ($t_{1/2}$) of the toxin/channel complex of 826 s. K_d calculated from the ratio k_{off}/k_{on} is 2.7 nM, a value close to that determined under equilibrium conditions.

[^{125}I]HgTX$_1$(A19Y/Y37F) Binding to KcsA−Kv1.3 Chimera. In the presence of 3 mM potassium, binding of [^{125}I]-HgTX$_1$(A19Y/Y37F) to the KcsA−Kv1.3 chimera is a saturable process, K_d = 29 pM and B_{max} = 9.0 fmol/ng of purified protein, (Figure 3A, Table 1). This B_{max} value is close to the theoretically expected value of 12.3 fmol/ng of protein. The K_d value is in good agreement with the K_i value of 69 pM, determined in competition experiments (data not shown). Crude membrane preparations that express KcsA−Kv1.3 protein displayed a similar K_d value, 48 pM (data not shown), suggesting that the affinity of KcsA−Kv1.3 for [^{125}I]-HgTX$_1$(A19Y/Y37F) did not critically change during the solubilization and the purification procedures.

The kinetics of [^{125}I]HgTX$_1$(A19Y/Y37F) binding to KcsA−Kv1.3 was also investigated (Figure 3C,D). [^{125}I]-HgTX$_1$(A19Y/Y37F) binds to KcsA−Kv1.3 according to a bimolecular, fully reversible reaction, with a k_{on} of 2.0×10^8 M^{-1} s^{-1} and a k_{off} of 0.0045 s^{-1}. The K_d calculated from the ratio of k_{off}/k_{on} is 22.5 pM, a value close to that determined under equilibrium binding conditions (Table 1).

[^{125}I]HgTX$_1$(A19Y/Y37F) Binding to KcsA−Kv1.3 Chimera: Modulation by Potassium. Binding of [^{125}I]HgTX$_1$-(A19Y/Y37F) to mammalian Kv1.X channels has been shown to be specifically stimulated in the presence of low concentrations of K^+ (*15*−*17*). Likewise, K^+ increases

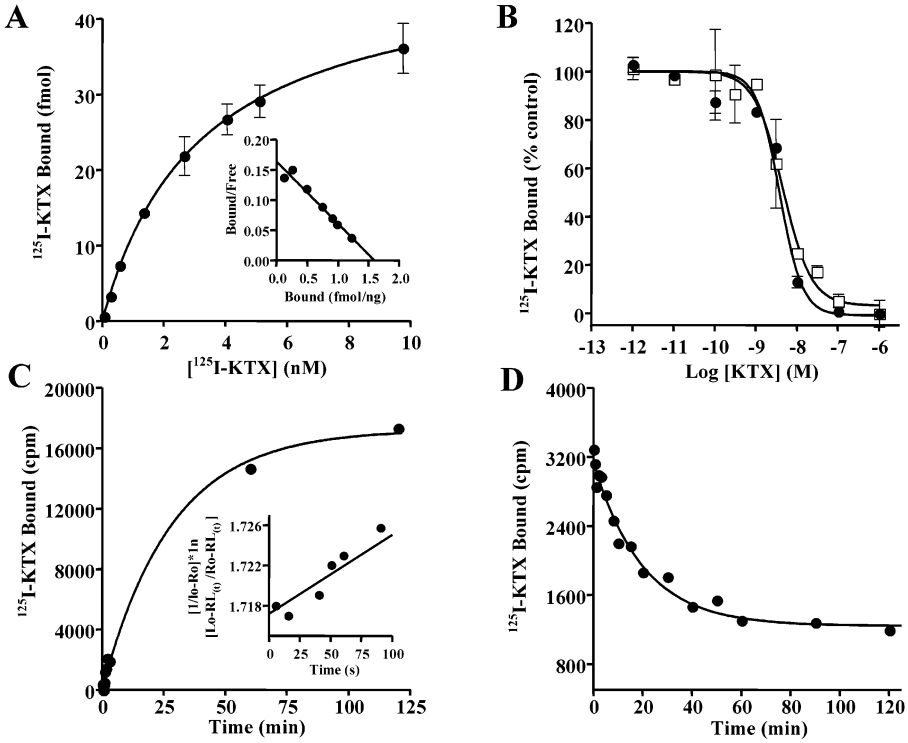

FIGURE 2: Characterization of [^{125}I]KTX binding to KcsA−Kv1.1 chimera. (A) Saturation binding isotherm. Purified KcsA−Kv1.1 was incubated with increasing concentrations of [^{125}I]KTX for 4 h at room temperature. Specific binding data were fitted to a single isotherm with a K_d of 3.2 nM and a B_{max} of 1.6 fmol/ng. Inset: Scatchard-plot representation of specific binding data. (B) Competition experiments. Crude *E. coli* membranes (●) or purified KcsA−Kv1.1 (□) were incubated with either 0.2 or 0.5 nM [^{125}I]KTX in the absence or presence of increasing concentration of synthetic unlabeled KTX. Crude membranes: IC_{50} = 3.8 nM, n_H = 1.57, K_i = 3.6 nM; purified channel: IC_{50} = 4.5 nM, n_H = 1.26, K_i = 3.9 nM. (C) Association kinetics. Purified KcsA−Kv1.1 was incubated with 50 pM [^{125}I]KTX for different periods of time. Inset: a semilogarithmic representation of the second-order association reaction, giving a k_{on} of 3.1×10^5 M^{-1} s^{-1}, calculated according to ref *17*. (D) Dissociation kinetics. After incubation of KcsA−Kv1.1 with 100 pM [^{125}I]KTX for 3 h at room temperature, unlabeled KTX was added to a final concentration of 100 nM. Bound ligand was determined at different periods of time. Data have been fitted to a single monoexponential decay corresponding to a first-order reaction with a k_{off} of 0.00083 s^{-1}.

specific binding of [^{125}I]$HgTX_1$(A19Y/Y37F) to KcsA−Kv1.3 with apparent halfmaximal stimulation occurring at 0.48 mM (Figure 3B). [^{125}I]$HgTX_1$(A19Y/Y37F) binding to KcsA−Kv1.3 was progressively reduced as K^+ concentration was raised above 2 mM, and no binding was observed in the presence of 100 mM K^+. Halfmaximal inhibition occurs in the presence of ∼12 mM potassium.

[^{125}I]$HgTX_1$(A19Y/Y37F) Binding to KcsA−Kv1.1, KcsA−Kv1.2, and KcsA−Kv1.6 Chimeras. Under equilibrium conditions, [^{125}I]$HgTX_1$(A19Y/Y37F) binds in a saturable fashion to KcsA−Kv1.1, KcsA−Kv1.2, and KcsA−Kv1.6 chimeras. Data were fitted to a single binding isotherm with a K_d of 0.42 nM and a B_{max} of 2.7 fmol/ng of purified KcsA−Kv1.1 protein, a K_d of 0.30 nM and a B_{max} of 11.4 fmol/ng of purified KcsA−Kv1.2 protein, and a K_d of 0.43 nM and a B_{max} of 10.9 fmol/ng of purified KcsA−Kv1.6 protein (Table 1). These K_d values are in good agreement with the respective K_i values (0.31 nM, 0.74 nM, and 0.66 nM for KcsA−Kv1.1, KcsA−Kv1.2, and KcsA−Kv1.6, respectively) determined in competition experiments (data not shown). KcsA−Kv1.1 and KcsA−Kv1.2 chimeras appear to have 5−10-fold lower affinity for [^{125}I]$HgTX_1$(A19Y/Y37F) as compared to KcsA−Kv1.3 (Table 1). The KcsA−Kv1.1, KcsA−Kv1.2, and KcsA−Kv1.3 chimeras bound [^{125}I]$HgTX_1$(A19Y/Y37F) with 1000-fold lower affinities as compared to the mammalian Kv1.1, Kv1.2, and Kv1.3 channels, whereas the difference in binding affinity between the KcsA−Kv1.6 chimera and the Kv1.6 channels is ∼30-fold lower affinity than (*9*). As observed with [^{125}I]KTX, the B_{max} value for the KcsA−Kv1.1 chimera is lower than the theoretically expected value, suggesting a stability problem with the purified chimera preparation.

SPR Analysis of Scorpion Toxin Interactions with KcsA−Kv1.3 Chimera.KcsA−Kv1.3 chimera was immobilized onto a commercially available CM5 dextran chip for use in a Biacore instrument to determine peptide binding by SPR (see Experimental Procedures). SPR analysis of binding reactions offers the advantage to detect the interactions of unlabeled molecules. Thus, the system represents an attractive alternative to radioactive ligand binding assays and can be used to study the kinetics of interaction of any ligand with a protein. To minimize nonspecific binding interactions of the peptides with the CM5 dextran chip surface, we used a media containing 150 mM NaCl. Under these conditions, CM5 dextran surfaces loaded with wild-type KcsA do not bind either KTX or $HgTX_1$ (data not shown). However, either peptide led to reproducible responses on a KcsA−Kv1.3 biosensor surface. The SPR signal of ∼120 resonance units (RU) was ∼30% of the maximum theoretical response of a fully active chimera, indicating successful immobilization of KcsA−Kv1.3.

The kinetics of KTX, ChTX, $HgTX_1$, and $HgTX_1$(A19Y/Y37F) binding to the KcsA−Kv1.3 chimera was determined. In the concentration range from 0.15−8 nM, we observed typical dose-dependent sensorgrams (Figure 4). A 1:1 Langmuir model with binding of the peptide to one receptor

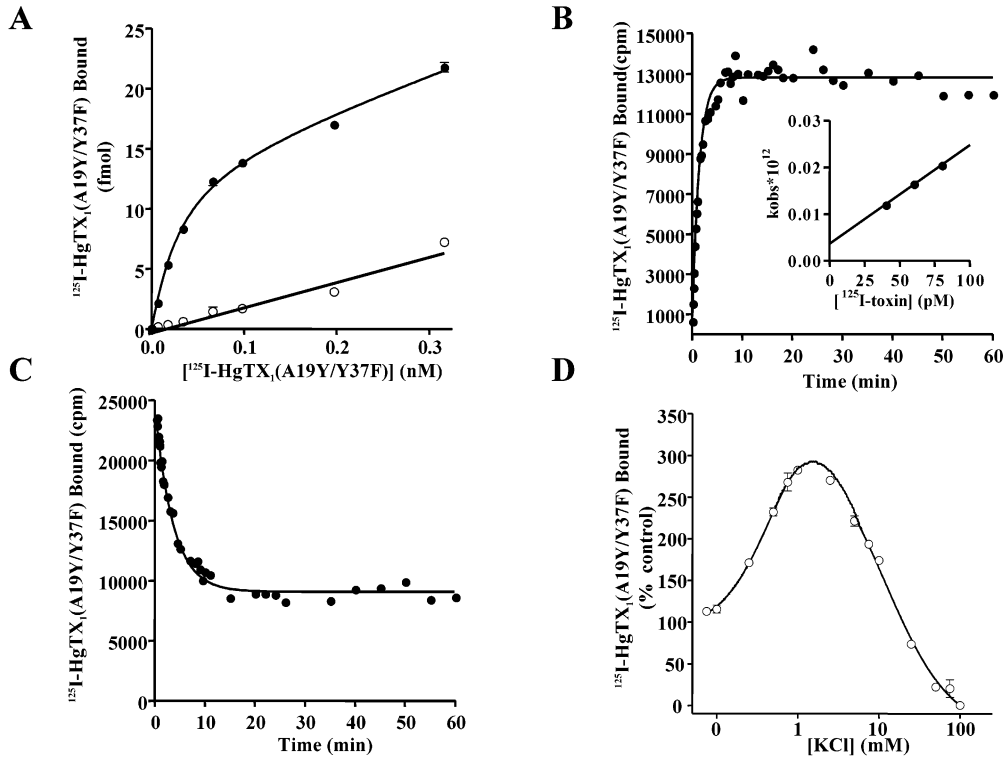

FIGURE 3: Characterization of [^{125}I]HgTX$_1$(A19Y/Y37F) binding to KcsA−Kv1.3 chimera. (A) Saturation binding isotherm. Purified KcsA−Kv1.3 was incubated with increasing concentrations of [^{125}I]HgTX$_1$(A19Y/Y37F) at room temperature for 2−3 h. In this case, depletion of the receptor occurred during binding. Binding data were fitted with a K_d of 29 pM and a B_{max} of 9 fmol/ng. (B) Association kinetics. Purified KcsA−Kv1.3 was incubated with 40 pM [^{125}I]HgTX$_1$(A19Y/Y37F) for the indicated periods of time. Nonspecific binding was determined in the presence of 100 nM unlabeled peptide and has been subtracted from the experimental data. Inset: k_{obs} values were determined from specific binding data at three different concentrations of [^{125}I]HgTX$_1$(A19Y/Y37F). $k_{on} = 2.0 \times 10^8$ M^{-1} s^{-1}. (C) Dissociation kinetics. After incubating KcsA−Kv1.3 with 50 pM [^{125}I]HgTX$_1$(A19Y/Y37F) for 2 h, ligand dissociation was initiated by addition of 100 nM unlabeled peptide, and incubation was followed at room temperature for different periods of time. $k_{off} = 0.0045$ s^{-1}. (D) Modulation of [^{125}I]HgTX$_1$(A19Y/Y37F) binding to KcsA−Kv1.3 channels by K^+ ions. Purified KcsA−Kv1.3 channels were incubated with 50 pM [^{125}I]HgTX$_1$(A19Y/Y37F) in the presence of increasing concentrations of KCl. Specific binding data were assessed relative to an untreated control (0 mM KCl) and fitted as described previously (*16*). K^+ modulated [^{125}I]HgTX$_1$(A19Y/Y37F) binding to KcsA−Kv1.3 with an $EC_{50} = 0.48$ mM ($n_{H1} = 1.39$) and an $IC_{50} = 11.5$ mM ($n_{H2} = 1.15$).

Table 1: Binding of [^{125}I]HgTX$_1$(A19Y/Y37F) to KcsA−Kv1.X Chimeras[a]

	KcsA−Kv1.X chimeras		native Kv1 channels
	K_d (pM)	B_{max} (fmol/ng)	K_i (pM)
KcsA−Kv1.1	423	2.7	0.12
KcsA−Kv1.2	297	11.4	0.09[b]
KcsA−Kv1.3	29	9.0	0.31
KcsA−Kv1.6	432	10.9	8.7[b]

[a] K_i and K_d values for [^{125}I]HgTX$_1$(A19Y/Y37F) binding to KcsA−Kv1.X chimeras were determined from competition and saturation experiments. K_i values for HgTX$_1$(A19Y/Y37F) binding to native Kv1 channels (*9*) have been included for comparison. [b] Data were obtained with HgTX$_1$ instead of HgTX$_1$(A19Y/Y37F).

site did not give a satisfying representation of experimental data. Careful inspection of the sensorgrams revealed participation of mass transfer, which should be expected for the range of estimated on-rates. Adding a mass transfer contribution to the 1:1 Langmuir model reduced significantly the deviation between data and fit. The kinetic constants for each peptide were calculated. KTX and ChTX displayed comparable association rate constants (k_{on} values of 1.5×10^7 and 8.9×10^6 M^{-1} s^{-1}, respectively). However, KTX dissociated 10-fold slower (k_{off} of 0.0038 s^{-1}, Figure 4A) than ChTX (k_{off} of 0.030 s^{-1}, Figure 4B). For HgTX$_1$ and its analogue, HgTX$_1$(A19Y/Y37F), the association rate constants were 2.6×10^6 (Figure 4C) and 6.3×10^6 M^{-1} s^{-1} (Figure 4D), respectively. HgTX$_1$ and HgTX$_1$(A19Y/Y37F) dissociated from the channel with k_{off} values of 0.007 and 0.008 s^{-1}, respectively. Both peptides displayed similar kinetic parameters in agreement with data obtained in filter binding experiments (*9*). The K_d values of KTX, ChTX, HgTX$_1$, and HgTX$_1$(A19Y/Y37F) calculated from ratios k_{off}/k_{on} were 0.28, 3.3, 2.8, and 1.3 nM, respectively. For KTX binding, the K_d value was in good agreement with the value determined in filter binding experiments using the purified KcsA−Kv1.3 chimera (see Table 1). In contrast, K_d for HgTX$_1$ binding, calculated from the kinetic experiments, was 1 order of magnitude higher than the K_d determined in filter binding experiments (Table 1). This shift resulted from a 100-fold slower on-rate and could be due to a difference in experimental conditions between the assays. It is well-established that the interaction of scorpion toxins with potassium channels is sensitive to the ionic strength of the media (*15*).

DISCUSSION

The bacterial channel, KcsA, is the only potassium channel for which a high-resolution crystal structure has been obtained (*3*, *4*). KcsA shares a remarkable structural homology in the pore region with eukaryotic potassium channels

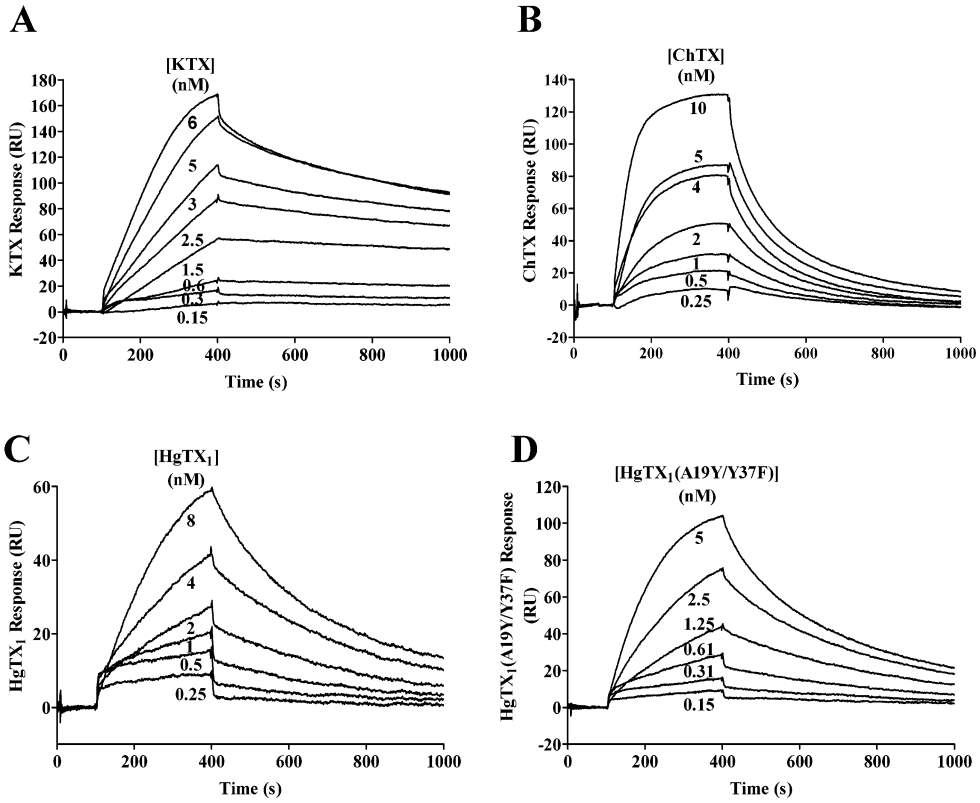

FIGURE 4: Binding of various peptides to a KcsA−Kv1.3 biosensor surface. Sensorgrams are shown illustrating the effect of injection of different concentrations of the following peptides: KTX (A), ChTX (B), $HgTX_1$ (C), and $HgTX_1$(A19C/Y37F) (D). Sensorgrams were fitted to a 1:1 Langmuir binding model, incorporating a mass transfer contribution. (A) $k_{on} = 1.5 \times 10^7$ M^{-1} s^{-1}, $k_{off} = 0.0038$ s^{-1}, and $k_t = 11 \times 10^7$ RU M^{-1} s^{-1}; (B) $k_{on} = 8.9 \times 10^6$ M^{-1} s^{-1}, $k_{off} = 0.03$ s^{-1}, and $k_t = 19 \times 10^7$ RU M^{-1} s^{-1}; (C) $k_{on} = 2.6 \times 10^6$ M^{-1} s^{-1}, $k_{off} = 0.007$ s^{-1}, and $k_t = 5 \times 10^7$ RU M^{-1} s^{-1}; (D) $k_{on} = 6.3 \times 10^6$ M^{-1} s^{-1}, $k_{off} = 0.008$ s^{-1}, and $k_t = 15 \times 10^7$ RU M^{-1} s^{-1}.

(*6*). This characteristic allowed the design of a high-affinity receptor site for the scorpion peptide KTX by substituting amino acids in the P region of KcsA with those of the human Kv1.3 channel (*7*). The results of this study demonstrated that specific pharmacological properties of other Kv1.X could be conferred to KcsA. Accordingly, we created a panel of chimeric KcsA−Kv1.X channels that contain the P region of hKv1.1, hKv1.2, hKv1.3, hKv1.4, hKv1.5, or hKv1.6 by substituting the residues of the turret region of KcsA with the corresponding residues of hKv1.1, hKv1.2, hKv1.3, hKv1.4, hKv1.5, and hKv1.6 (subregion I or SIP region in Figure 1A). The chimeras were expressed and purified as tetrameric proteins. The results of binding experiments with [^{125}I]KTX and [^{125}I]$HgTX_1$(A19Y/Y37F) indicate that the KcsA−Kv1.X chimeras can reproduce the pharmacological profiles of mammalian Kv1 channels. Thus, the affinity of KTX for KcsA−Kv1.3 is higher than for KcsA−Kv1.1, in agreement with functional data (*8*). Furthermore, [^{125}I]-$HgTX_1$(A19Y/Y37F) displays higher affinity for KcsA−Kv1.3 and KcsA−Kv1.1 than for KTX, as observed with native channels (*9*). The data support the notion that the SIP region in Kv1 channels represents an essential interaction surface for the binding of pore-blocking peptides. The interacting surface of the pore-blocking peptides in KcsA has been reported to be ~228 Å^2 (*6*). Three amino acid substitutions in this region are sufficient to render KcsA sensitive to agitoxin2 (*6*). Using our previous model for the interaction of KTX with chimeric KcsA−Kv1.3 channels (*7*), we examined the interacting molecular surface of the peptide and channel. The receptor site may be confined to a region between residues 56 and 64 (Figure 1A). Within this region, only four residues (at positions 56, 57, 58, and 64) appear to be in close contact with the peptide. Our results also show that the structural differences in this region between Kv1 channels determine the distinct pharmacological profile of these channels to the peptides.

While the SIP region appears to be essential to generate a specific receptor site in KcsA, native channels display a higher affinity for $HgTX_1$ than for KcsA−Kv1.X (*9*). Other parts of the pore region or other regions of the channel may also contribute to the toxin/channel interaction. This may explain why [^{125}I]$HgTX_1$(A19Y/Y37F) binds to KcsA−Kv1.1 and KcsA−Kv1.2 with a 10-fold lower affinity than to KcsA−Kv1.3, while the affinities for the corresponding Kv1.X channels differ only by a factor of 3 (Table 1). In addition, we can also not exclude subtle local structural differences between the KcsA pore region and that of Kv channels, as it has been reported (*18*). This possibility is also consistent with the differences in K^+ sensitivity between KcsA−Kv1.X and mammalian Kv1.X channels. Thus, binding of [^{125}I]$HgTX_1$(A19Y/Y37F) to KcsA−Kv1.3 is activated by low millimolar concentrations of potassium, as it has been observed to occur in other Kv1.X channels (*15*−*17*). However, [^{125}I]$HgTX_1$(A19Y/Y37F) binding to KcsA−Kv1.3 can occur in the absence of potassium, but potassium is required for scorpion toxin binding to mammalian Kv1.3 channels (*9*, *15*).

In this study, we have also shown data suggesting that SPR analysis can be applied to immobilized potassium channels for studying binding of peptides, such as those

derived from scorpion venoms. The tetrameric KcsA−Kv1.3 chimera remains active on the sensor surface, allowing the determination of binding events of high affinity in real time. About one-third of immobilized KcsA−Kv1.3 channels were accessible for peptide binding. Although the procedure used to immobilize KcsA−Kv1.3 on the CM5-dextran surface may have caused inactivation of some channels, binding data indicate that the inactive protein does not interfere with peptide binding to active KcsA−Kv1.3 chimeras. Recent improvements in the SPR technology (*19*−*21*) should allow the detection of small molecules (∼500 Da) binding to KcsA−Kv1.X biosensors. Thus, these systems have the potential of being used for screening complex mixtures of compounds, such as animal venoms, combinatorial peptide libraries, and small organic compound libraries. In conclusion, KcsA−Kv1.X biosensors have the potential of becoming substrates for high throughput assays designed toward the identification of novel potassium channel modulators of therapeutic interest.

ACKNOWLEDGMENT

We would like to thank Annette Marquardt, Monika Schmidt, and Iris Meier for excellent technical assistance and Dr. Pascale Marchot for continuous discussion during the course of this work. We also thank Dr. Gregory J. Kaczorowski for critical reading of the manuscript.

REFERENCES

1. Hille, B. (2001) *Ionic channel of excitable membranes*, 3rd ed., Sinauer Associates, Inc., Sunderland, MA.
2. Ashcroft, F. M. (2000) *Ion channels and disease*, Academic Press, New York.
3. Doyle, D. A., Morais, C. J., Pfuetzner, R. A., Kuo, A., Gulbis, J. M., Cohen, S. L., Chait, B. T., and Mackinnon, R. (1998) *Science 280*, 69−77.
4. Zhou, Y., Morais-Cabral, J. H., Kaufman, A., and Mackinnon, R. (2001) *Nature 414*, 43−48.
5. Pongs, O., and Legros, C. (2000) in *Handbook of Experimental Pharmacology* (Endo, M., and Mishina, M., Eds.) pp 177−196, Springer-Verlag, Berlin and Heidelberg.
6. Mackinnon, R., Cohen, S. L., Kuo, A., Lee, A., and Chait, B. T. (1998) *Science 280*, 106−109.
7. Legros, C., Pollmann, V., Knaus, H. G., Farrell, A. M., Darbon, H., Bougis, P. E., Martin-Eauclaire, M. F., and Pongs, O. (2000) *J. Biol. Chem. 275*, 16918−16924.
8. Grissmer, S., Nguyen, A. N., Aiyar, J., Hanson, D. C., Mather, R. J., Gutman, G. A., Karmilowicz, M. J., Auperin, D. D., and Chandy, K. G. (1994) *Mol. Pharmacol. 45*, 1227−1234.
9. Koschak, A., Bugianesi, R. M., Mitterdorfer, J., Kaczorowski, G. J., Garcia, M. L., and Knaus, H. G. (1998) *J. Biol. Chem. 273*, 2639−2644.
10. Laemmli, U. K. (1970) *Nature 227*, 680−685.
11. Romi, R., Crest, M., Gola, M., Sampieri, F., Jacquet, G., Zerrouk, H., Mansuelle, P., Sorokine, O., Van Dorsselaer, A., and Rochat, H. (1993) *J. Biol. Chem. 268*, 26302−26309.
12. Swillens, S. (1995) *Mol. Pharmacol. 47*, 1197−1203.
13. Schulze, C. (2000) *Recent research developments in comparative biochemistry and physiology*, Transworld Research Network, Trivandrum, India.
14. Karlsson, R., Michaelsson, A., and Mattsson, L. (1991) *J. Immunol. Methods 145*, 229−240.
15. Helms, L. M., Felix, J. P., Bugianesi, R. M., Garcia, M. L., Stevens, S., Leonard, R. J., Knaus, H. G., Koch, R., Wanner, S. G., Kaczorowski, G. J., and Slaughter, R. S. (1997) *Biochemistry 36*, 3737−3744.
16. Vazquez, J., Feigenbaum, P., King, V. F., Kaczorowski, G. J., and Garcia, M. L. (1990) *J. Biol. Chem. 265*, 15564−15571.
17. Knaus, H. G., Koch, R. O., Eberhart, A., Kaczorowski, G. J., Garcia, M. L., and Slaughter, R. S. (1995) *Biochemistry 34*, 13627−13634.
18. Wrisch, A., and Grissmer, S. (2000) *J. Biol. Chem. 275*, 39345−39353.
19. McDonnell, J. M. (2001) *Curr. Opin. Chem. Biol. 55*, 572−577.
20. Rich, R. L., Hoth, L. R., Geoghegan, K. F., Brown, T. A., LeMotte, P. K., Simons, S. P., Hensley, P., and Myszka, D. G. (2002) *Proc. Natl. Acad. Sci. U.S.A. 99*, 8562−8567.
21. Mizushina, Y., Kamisuki, S., Kasai, N., Shimazaki, N., Takemura, M., Asahara, H., Linn, S., Yoshida, S., Matsukage, A., Koiwai, O., Sugawara, F., Yoshida, H., and Sakaguchi, K. (2002) *J. Biol. Chem. 277*, 630−638.

BI026264A